

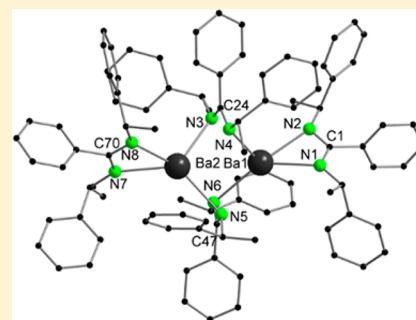
Homoleptic Chiral Benzamidinate Complexes of the Heavier Alkaline Earth Metals and the Divalent Lanthanides

Meng He, Michael T. Gamer, and Peter W. Roesky*

Institut für Anorganische Chemie, Karlsruher Institut für Technologie (KIT), Engesserstr. 15, 76131 Karlsruhe, Germany

S Supporting Information

ABSTRACT: Reaction of the chiral amidine *N,N'*-bis(1-phenylethyl)benzamidinate ((*S*)-HPEBA), $\text{KCH}(\text{SiMe}_3)_2$, and Ml_2 ($\text{M} = \text{Ca}, \text{Sr}, \text{Ba}$) or LnI_2 ($\text{Ln} = \text{Eu}, \text{Yb}$) in a 2:2:1 stoichiometric ratio resulted in the chiral homoleptic monomeric alkaline earth metal compounds $[\text{Ca}(\text{PEBA})_2(\text{THF})_2]$ (**1**) and $[\text{Sr}(\text{PEBA})_2(\text{THF})_2]$ (**2**), the dimeric barium complex $[\text{Ba}(\text{PEBA})_2]_2$ (**3**), and the monomeric divalent lanthanide compounds $[\text{Eu}(\text{PEBA})_2(\text{THF})_2]$ (**4**), and $[\text{Yb}(\text{PEBA})_2(\text{THF})_2]$ (**5**). The solid-state structures of all compounds were established by single-crystal X-ray diffraction. Three different structures are observed in the solid state. Compounds **1**, **2**, **4**, and **5** form distorted coordination octahedra. For the alkaline earth element complexes **1** and **2**, the two THF molecules are located in a *trans*-position, whereas, for the lanthanide compounds **4** and **5**, they are arranged in a *cis*-position. In contrast, the barium complex **3** is dimeric with two amidinate ligands in an unusual “side-on” bridging mode. All five complexes were used as catalysts for hydrophosphination reactions of styrene and substituted analogues.

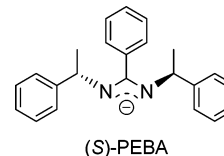


INTRODUCTION

Amidines and the closely related guanidines are a very popular class of ligands in organometallic and coordination chemistry. These monoanionic heteroallylic ligands coordinate to almost all metals of the periodic table.^{1–3} In most cases, a *N,N'*-chelating binding mode is observed.^{4–11} The broad application of amidines is a result of the good adjustability of these ligands. The amidinate anions of the general formula $[\text{RC}(\text{NR}')_2]^-$ allow an effective tuning of the steric and electronic requirements by varying the substituents *R* and *R'*. There are several synthetic strategies for the access of amidinate complexes reported,⁹ but for the lanthanides, either salt metathesis reactions of an alkali metal amidinate with a metal halide or deprotonation of an amidine with metal alkyls or amides is most common. However, other routes such as the insertion of carbodiimides into a metal–carbon bond are also known.

Since the pioneering work of Edelman et al.^{4–7,9–12} and later by Deacon and Junk et al.,^{13–16} amidines are very well established as ligands in rare-earth metal chemistry. In contrast, only a few structurally characterized amidinate compounds of the heavier alkaline earth metals (*Ca*, *Sr*, *Ba*) have been reported.^{17–24} Most of them were synthesized by Westerhausen et al.^{17–19,21,22} and Junk et al.^{23,24}

In contrast to the vast number of amidinate complexes, there are surprisingly few compounds with a chiral version of this ligand known.^{25–32} Before we entered the field, only relatively few complexes of group 4 metals,^{25–28} molybdenum,^{29,32} nickel,^{29,30} and rhodium^{31,32} with chiral amidinate ligands were reported. We recently published the first rare-earth metal complexes using the chiral amidinate *N,N'*-bis(1-phenylethyl)-benzamidinate ((*S*)-PEBA) as ligand (Scheme 1).^{33–36} The

Scheme 1. Chiral Amidinate ((*S*)-PEBA)

corresponding chiral amidine *N,N'*-bis(1-phenylethyl)-benzamidinate (HPEBA) was reported about 35 years ago by Brunner for the first time.²⁹ In our work, we developed an improved synthesis of HPEBA, including its single crystal structure and its corresponding lithium and potassium salts (LiPEBA and KPEBA).³³

In trivalent lanthanide chemistry, we synthesized the tris(amidinate) complex $[\{(\text{S})\text{-PEBA}\}_3\text{Sm}]$, the bis(amidinate) complexes $[\text{Ln}(\text{PEBA})_2(\mu\text{-Cl})_2]$ ($\text{Ln} = \text{Sm}, \text{Er}, \text{Yb}, \text{Lu}$), and the mono(amidinate) compounds $[\text{Ln}(\text{PEBA})(\text{Cl})_2(\text{THF})_n]$ ($\text{Ln} = \text{Sm}, \text{Yb}, \text{Lu}$).^{34,35} Furthermore, the chiral mono(amidinate) bisborohydride rare-earth complexes $[\text{Ln}\{(\text{S})\text{-PEBA}\}(\text{BH}_4)_2(\text{THF})_2]$ ($\text{Ln} = \text{Sc}, \text{La}, \text{Nd}, \text{Sm}, \text{Yb}$), *Lu*) were prepared.³⁶ The chiral bis(amidinate) amido complexes $[\{(\text{S})\text{-PEBA}\}_2\text{Ln}\{\text{N}(\text{SiMe}_3)_2\}]$ ($\text{Ln} = \text{Y}, \text{Lu}$) were used as precatalysts in the enantioselective hydroamination/cyclization reaction. Good catalytic activities and high enantioselectivities were observed.^{34,35}

The addition of a P–H function across an unactivated carbon–carbon double or triple bond (hydrophosphination) is an attractive route for the synthesis of phosphines.^{37–40} It is

Received: May 9, 2016

related to the above-mentioned hydroamination. Intramolecular hydrophosphination of alkynes catalyzed by trivalent lanthanides was reported 15 years ago by Marks et al.^{41–44} The first intermolecular version using divalent lanthanides followed soon thereafter.⁴⁵ Ever since, there is an increasing interest in the hydrophosphination catalyzed by di- and trivalent lanthanide complexes.^{46–52} The recent development was covered by some review articles.^{53–57}

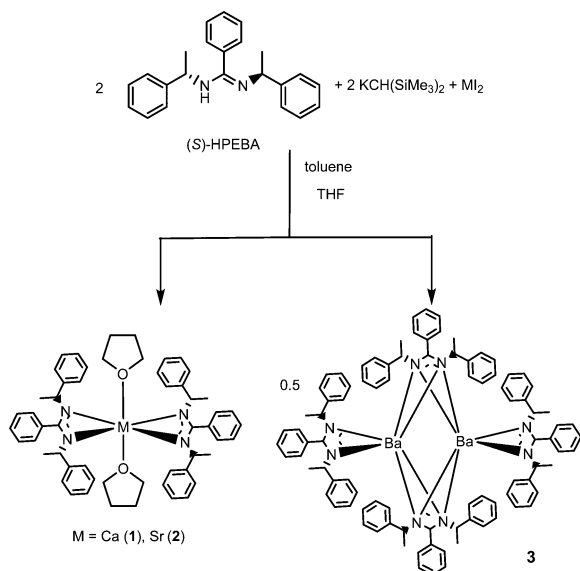
As reported earlier, the reactivity and coordination behavior of divalent lanthanide complexes and the heavier alkaline earth metals is in some cases similar.^{58–61} This relationship in coordination chemistry originates from the similar ion radii (for CN 6 (pm): Ca²⁺ 100, Yb²⁺ 102, Sr²⁺ 118, Eu²⁺ 117).⁶² In terms of σ -bond metathesis, there is also a certain similarity between group 2 elements, which have a d⁰ electronic configuration and the trivalent redox inactive d⁰ lanthanide complexes.⁶³ As a result of this chemical relationship, the heavier alkaline earth metals have also been employed recently as catalysts for the hydrophosphination reaction.^{46,50,63–66} Usually, the order of reactivity was found to be Ca < Sr < Ba.^{46,63,66}

Herein, we describe the synthesis and characterization of chiral homoleptic (S)-PEBA complexes of divalent lanthanide and the heavier alkaline earth elements as well as their application as catalyst in the hydrophosphination reaction.

RESULTS AND DISCUSSION

Reaction of (S)-HPEBA, KCH(SiMe₃)₂, and MI₂ (M = Ca, Sr, Ba) in a 2:2:1 stoichiometric ratio resulted in the chiral homoleptic monomeric alkaline earth metal compounds [Ca(PEBA)₂(THF)₂] (1) and [Sr(PEBA)₂(THF)₂] (2) and in the dimeric barium complex [Ba(PEBA)₂]₂ (3) (Scheme 2).

Scheme 2. Synthesis of 1–3



In the first step, (S)-HPEBA is treated with KCH(SiMe₃)₂ to give (S)-KPEBA, which is then reacted in a salt metathesis with MI₂ to give the desired complexes in moderate yields as single crystalline material. These single crystals were obtained from a concentrated *n*-pentane solution. Compounds 1 and 2 are monomeric complexes, in which two (S)-PEBA ligands and two molecules of THF coordinate to the metal center. In contrast,

the larger barium atoms in 3 each are coordinated by one terminal and two metal bridging (S)-PEBA ligands.

Compounds 1–3 were fully characterized by standard analytical/spectroscopic techniques, and their solid-state structures were established by single-crystal X-ray diffraction. In the ¹H NMR spectra, the signal of the methyl group, which split into a doublet, and the methine group, which appears as multiplet, are characteristic. For the calcium compound 1 (Figure S1), the signals are well resolved (δ = 1.47 (CH₃), 4.29 (NCH)), whereas they are broadened for compound 2 (δ = 1.44 (CH₃), 4.29 (NCH)) (Figure S3). These signals are slightly shifted in comparison to those of KPEBA (δ = 1.30 (CH₃) and 4.22 ppm (NCH)).³³ For the barium complex, two different amidinate ligands (terminal and metal bridging) are seen. Therefore, two sets of signals for the amidinate ligands were observed in the ¹H and ¹³C{¹H} NMR spectra (Figures S5 and S6), e.g., at δ (¹H) = 1.14 and 1.25 for the CH₃ groups. In the IR spectrum, a characteristic strong peak at 1636 cm^{–1}, which is assigned to the carbon–nitrogen stretching vibration, is observed for each compound.

The monomeric complexes 1 and 2 are isostructural (Figure 1). They crystallize in the chiral tetragonal space group P4₁2₁

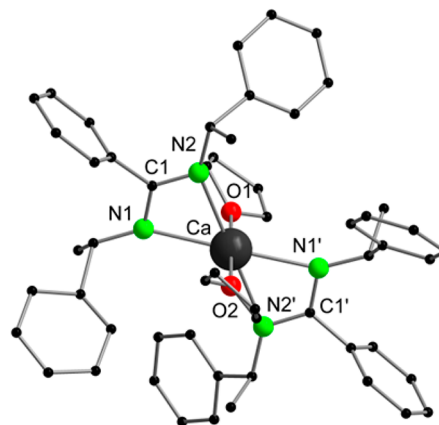


Figure 1. Molecular structure of 1 in the solid state, omitting the hydrogen atoms for clarity. Selected bond lengths [Å] or angles [deg] (data for the isostructural compound 2 are also given). 1: Ca–N1 2.443(2), Ca–N2 2.448(2), Ca–C1 2.849(2), Ca–O1 2.421(3), Ca–O2 2.373(3), N1–C1 1.325(3), N1–C9 1.42(2), N2–C1 1.323(3), C1–C2 1.476(8); N1–Ca–N2 55.28(6), N1–Ca–N1' 177.37(12), N1–Ca–O1 88.68(6), N1–Ca–O2 91.32(6), N1–C1–N2 117.9(2), N2–Ca–O1 90.41(6), N2–Ca–O2 89.59(6), N2–Ca–N2' 179.18(12), O1–Ca–C1 89.81(6), O2–Ca–C1 90.19(6), O1–Ca–O2 180.00(4). 2: Sr–N1 2.567(3), Sr–N2 2.578(3), Sr–C1 2.995(3), Sr–O1 2.546(4), Sr–O2 2.507(5), N1–C1 1.326(4), N1–C9 1.44(2), N2–C1 1.329(4), C1–C2 1.496(7); N1–Sr–N2 52.40(9), N1–Sr–N1' 177.0(2), N1–Sr–O1 88.50(8), N1–Sr–O2 91.50(8), N1–C1–N2 117.6(3), N2–Sr–O1 90.54(9), N2–Sr–O2 89.46(9), N2–Sr–N2' 179.0(2), O1–Sr–C1 89.65(8), O2–Sr–C1 90.35(8), O1–Sr–O2 180.00(3).

with half of a molecule in the asymmetric unit. A crystallographic C₂ axis is located through the center metal. Although some disorder is observed, the structures were fully refined. Each metal atom is 6-fold coordinate by two chelating amidinate ligands and two molecules of THF. A distorted coordination octahedron around the alkaline earth metal is observed. The two THF molecules are located in a *trans*-position with an ideal angle of 180°. As a result of the tight NCN bite angle of 117.9(2)° (1) and 117.6(3)° (2), the

octahedron is distorted. The M–N bond distances of each ligand are almost identical, showing Ca–N bond lengths of 2.443(2) and 2.448(2) Å and Sr–N bond lengths of 2.567(3) and 2.578(3) Å. A similar distorted octahedral arrangement is observed in other achiral amidinate complexes of the alkaline earth metals, e.g., in calcium and strontium bis[*N,N'*-bis(trimethylsilyl)benzamidinate]·2THF, also a *trans*-coordination of the THF molecules was seen.^{17,19}

Compound 3 crystallizes in the chiral orthorhombic space group $P2_12_12_1$ with one molecule of 3 and one molecule of *n*-pentane in the asymmetric unit (Figure 2). The bimetallic

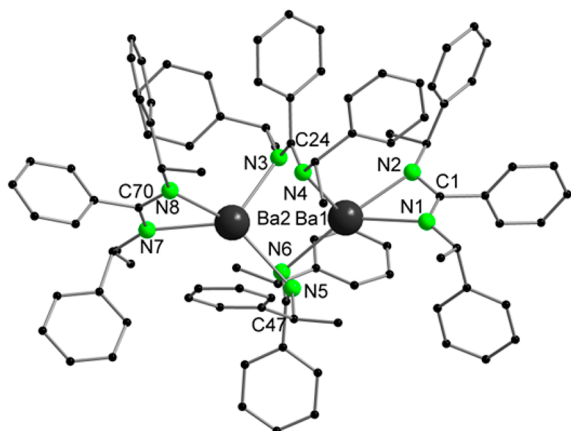
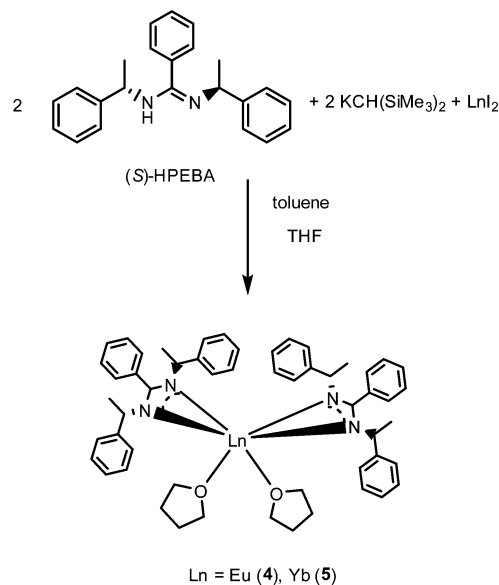


Figure 2. Molecular structure of 3 in the solid state, omitting the hydrogen atoms and the solvent molecules for clarity. Selected bond lengths [Å] or angles [deg]: Ba1–N1 2.740(3), Ba1–N2 2.711(3), Ba1–N3 2.900(3), Ba1–N4 2.782(3), Ba1–C1 3.120(4), Ba1–C24 3.154(3), Ba1–C47 3.301(3), Ba1–Ba2 3.8231(3), Ba2–N3 2.876(3), Ba2–N4 2.905(3), Ba2–N7 2.764(3), Ba2–N8 2.706(3), Ba2–C70 3.158(4), N1–Ba1–N2 49.68(10), N3–Ba1–N4 46.81(9), N5–Ba2–N6 45.36(9), N7–Ba2–N8 49.57(9), C1–Ba1–Ba2 162.55(8), Ba1–Ba2–C70 168.70(8).

compound shows an unusual coordination mode of the amidinate ligands. Whereas two of those ligands coordinate in the expected chelating mode, the other two amidinate ligands bridge the barium atoms in a “side-on” fashion in a μ^2, κ^2-N, N' -bridging mode. This coordination mode is very rare. To the best of our knowledge, such a structural motif was not observed earlier in barium amidinate chemistry. However, an amidinate bridging a barium and potassium atom was reported in $[\{\text{PhC}\equiv\text{CC}(\text{NiPr})_2\}_3\text{BaK}]_n$.⁶⁷ A structure related to 3 was observed in the guanidinate complex $[(\text{L})\text{Ba}(\mu^2\text{-L})_2\text{Ba}(\text{L})]$ (HL = $i\text{PrN}=\text{C}(\text{N}(i\text{Pr})_2)\text{N}(\text{H})i\text{Pr}$).⁶⁸ In 3, each barium atom is 6-fold coordinate. The coordination geometry around the Ba atom is best described as a distorted trigonal prism. No solvent molecule is bound to the metal center. The Ba–N bond lengths of the bridging ligands are not equivalent (Ba1–N3 2.900(3) Å, Ba2–N3 2.876(3) Å, Ba1–N4 2.782(3) Å, Ba2–N4 2.905(3) Å, Ba1–N5 3.130(3) Å, Ba2–N5 2.871(3) Å, Ba1–N6 2.837(3) Å, Ba2–N6 3.025(3) Å). They are slightly longer than the Ba–N bond lengths of terminal ligands (Ba1–N1 2.740(3) Å, Ba1–N2 2.711(3) Å, Ba2–N7 2.764(3) Å, Ba2–N8 2.706(3) Å). The bite angles of the bridging ligands (N3–Ba1–N4 46.81(9)°, N5–Ba1–N6 44.55(9)°, N3–Ba2–N4 46.81(9)°, N5–Ba2–N6 45.36(9)°) are smaller than those of the terminal ones (N1–Ba1–N2 49.68(10)°, N7–Ba2–N8 49.57(9)°).

In a similar approach as that used for the synthesis of 1–3, the homoleptic divalent lanthanide complexes $[\text{Eu}(\text{PEBA})_2(\text{THF})_2]$ (4) and $[\text{Yb}(\text{PEBA})_2(\text{THF})_2]$ (5) were obtained. Reaction of (S)-HPEBA, $\text{KCH}(\text{SiMe}_3)_2$, and LnI_2 (Ln = Eu, Yb) in a 2:2:1 stoichiometric ratio resulted in the desired chiral compounds (Scheme 3). Although the synthesis is similar to

Scheme 3. Synthesis of 4 and 5



the alkaline earth compounds, the solid-state structures of 4 and 5 are different. Compounds 4 and 5 crystallize in the orthorhombic space group $P2_12_12_1$ with one molecule of the complex in the asymmetric unit (Figure 3). Both compounds

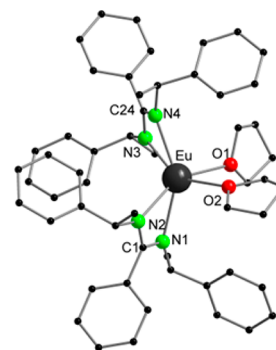


Figure 3. Molecular structure of 4 in the solid state, omitting the hydrogen atoms for clarity. Selected bond lengths [Å] or angles [deg] (data for the isostructural compound 5 are also given). 4: Eu–N1 2.582(4), Eu–N2 2.567(4), Eu–N3 2.557(4), Eu–N4 2.580(3), Eu–C1 2.995(5), Eu–C24 2.987(5), Eu–O1 2.600(3), Eu–O2 2.613(4); N1–Eu–N2 52.67(13), N1–Eu–N3 107.45(13), N1–Eu–N4 148.33(14), N1–Eu–O1 102.00(13), N1–Eu–O2 101.70(14), N3–Eu–N4 52.74(15), N3–Eu–O1 83.7(2), N3–Eu–O2 148.18(14), N4–Eu–O1 99.89(12), N4–Eu–O2 105.1(2), O1–Eu–O2 77.9(2). 5: Yb–N1 2.475(3), Yb–N2 2.470(3), Yb–N3 2.452(3), Yb–N4 2.483(2), Yb–C1 2.881(4), Yb–C24 2.871(3), Yb–O1 2.491(3), Yb–O2 2.505(3); N1–Yb–N2 55.02(9), N1–Yb–N3 108.36(10), N1–Yb–N4 152.31(10), N1–Yb–O1 101.61(10), N1–Yb–O2 100.10(10), N3–Yb–N4 55.07(10), N3–Yb–O1 83.23(10), N3–Yb–O2 148.35(10), N4–Yb–O1 98.22(9), N4–Yb–O2 102.89(10), O1–Yb–O2 77.65(10).

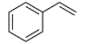
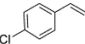
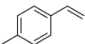
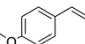
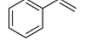
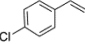
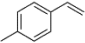
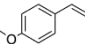
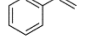
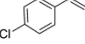
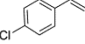
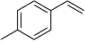
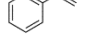
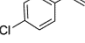
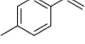
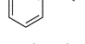
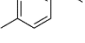
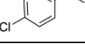
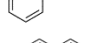
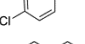
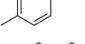
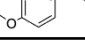
are isostructural. As observed for **1** and **2**, monometallic complexes were formed, in which the metal center is surrounded by two (*S*)-PEBA ligands and two molecules of THF. In contrast to **1** and **2**, the stereochemistry of the thus obtained distorted coordination octahedron is different. The THF molecules in **4** and **5** are arranged in a *cis*-position with an O1–Ln–O2 angle of 77.9(2)° (**4**) and 77.65(10)° (**5**). There are surprisingly only very few structurally characterized bis(amidinate) complexes of the divalent lanthanides known. In ytterbium bis[*N,N'*-bis(trimethylsilyl)benzaminate]·2THF, a *trans*-coordination of the THF molecules was seen.¹² In contrast, the lanthanide(II)bis(amidinate) complexes [LnL₂·(THF)₂] (Ln = Sm, Eu; L = PhC(NSiMe₃)(NC₆H₃iPr₂-2,6)) show a *cis*-configuration for samarium and both *cis*- and *trans*-configurations for europium.⁶⁹ For the lanthanide(II)bis(guanidinate) complexes, [Ln(Giso)₂] (Ln = Sm, Eu; Giso = [(ArN)₂CN(C₆H₁₁)₂][–], Ar = 2,6-diisopropylphenyl), planar 4-coordinate samarium and europium atoms and distorted tetrahedral coordinate ytterbium atoms were reported.⁷⁰ In contrast, the homoleptic four-coordinate lanthanide(II) complexes [Ln(Priso)₂] (Ln = Sm, Eu, Yb; Priso = [(ArN)₂CN(Pr)₂][–], Ar = 2,6-diisopropylphenyl) show coordination geometries midway between tetrahedral and planar.⁷¹ The Ln–N bond distances in **4** and **5** are in the expected ranges of 2.557(4)–2.582(4) Å (compound **4**) and 2.452(3)–2.483(2) Å (compound **5**).

The diamagnetic complex **5** was also characterized by NMR spectroscopy (Figures S7–S9). In the ¹H NMR spectrum, the signals of the methyl (δ = 4.40 ppm) and the methine group (δ = 1.39 ppm) of (*S*)-PEBA are well resolved. A 2D ¹H, ¹⁷¹Yb-gHMBC NMR spectrum (gradient-selected Heteronuclear Multiple-Bond Coherence) shows a ¹⁷¹Yb peak at 792 ppm, which couples to the NCH group of the ligand (Figure S9).

Compounds **1–5** were used as precatalysts in the hydrophosphination reaction of differently substituted styrenes and Ph₂PH (Table 1). In contrast to the well-established hydrophosphination catalysts of the alkaline earth metals, compounds **1–5** do not have a leaving group.^{46,50,63–66,72} Attempts to synthesize compounds with a leaving group, e.g., [M((*S*)-PEBA)CH(SiMe₃)₂], failed. We presume that this is a result of the Schlenk equilibrium. Nevertheless, we used **1–5** as Lewis acidic catalysts. As a result of the low pK_a values of phosphines, we do not anticipate a substitution of one (*S*)-PEBA ligand by a phosphine during the catalytic transformation. To support this assumption, we reacted **5** and Ph₂PH in a 1:1 ratio (Figure S24). There is no sign of ligand displacement or oxidation of the ytterbium atom, which would result in a paramagnetic sample. Moreover, a 2D ¹H, ¹⁷¹Yb-gHMBC NMR spectrum of **5** in the presence of Ph₂PH was recorded (Figure S25). As expected, no ¹⁷¹Yb, ³¹P coupling, and thus no tight coordination, was observed.

The products of the catalytic hydrophosphination were obtained in moderate to high yield and high purity. With one exception, all reactions were conducted with 2.5 or 5 mol% catalyst loading in benzene at 60 °C in NMR scale. The transformation of *p*-chlorostyrene in the presence of **3** was also performed at room temperature (Table 1, entry 10). The reaction was monitored by NMR spectroscopy. Conversions were calculated based on the integration area of product and starting material signals in the ¹H and ³¹P{¹H} NMR spectra. Although the ³¹P NMR spectrum was recorded in a proton decoupled mode, the results do not deviate significantly from the results obtained by ¹H NMR spectroscopy. In ³¹P{¹H}

Table 1. Intermolecular Hydrophosphination of Styrenes with Diphenylphosphine

$\text{R-CH=CH}_2 + \text{HPPH}_2 \xrightarrow[60\text{ }^\circ\text{C}]{5\text{ mol\% cat.}} \text{R-CH}_2\text{CH}_2\text{PPh}_2$				
entry	cat.	substrate	t/ h	conv. ^a / %
1.	1		84	54
2.			118	58
3.			98	39
4.			90	47
5.	2		64	76
6.			94	78
7.			120	45
8.			110	40
9 ^b	3		6.5	97
10 ^{b,c}			36	77
11 ^b			3	96
12 ^b			48	77
13.	4		64	83
14.			48	91
15.			120	25
16.	5		95	85
17.			92	77
18.			– ^d	– ^d
19.	none		105	25
20.			101	27
21.			101	25
22.			135	33

^aBased on the consumption of diphenylphosphine from integration of signals in the ³¹P{¹H} NMR. ^b2.5 mol% catalyst used. ^cAmbient temperature. ^dDecomposition of the catalyst.

NMR spectra, the peak at δ = –40 ppm was assigned to the starting material diphenylphosphine, while the new peak at around δ = –20 ppm belongs to the hydrophosphination products. Blank reactions without catalysts have been performed for comparison (Table 1, entries 19–22). Even without a catalyst, formation of the hydrophosphination products was observed at high temperature over a long period.

It can be clearly seen from Table 1 that the yields and the reaction times are substrate and catalyst dependent. Most of the

catalytic reactions stopped before being completed. Within the series of the heavier alkaline earth metals 1–3, the barium compound 3 showed the highest activity (entries 9–12). Since compound 3 is bimetallic, we used in comparison to the other catalyst only half of the stoichiometric amount to have the same molar concentration of the metal atoms. By using a catalyst loading of 2.5 mol% of 3 and *p*-chlorostyrene as substrate, the corresponding product even formed at room temperature in 36 h, achieving a conversion of 77% (entry 10). At 60 °C, the *p*-chlorostyrene can be converted within 3 h to a conversion of 94%. In contrast, the same reaction occurred with conversions of only 58% (118 h) and 78% (94 h) by using 1 and 2 as catalysts, respectively (entries 2 and 6). As observed earlier in hydrophosphination reaction, the catalyst activity increased with increasing ion radius of the center metal.^{46,63,66} In fact, there is, in some cases, not a significant improvement by using 1 as a catalyst (entries 1–4) in comparison to the blank reaction (entries 19–22). Cooperative effects of the bimetallic compound 3 do not seem to play a significant role.

Next, we investigated the divalent lanthanide compounds 4 and 5 as catalysts. For styrene, the catalytic activities of 4 and 5 were comparable to those of 2 (entries 5, 13, and 16). However, 4 showed significantly better activity within a shorter reaction time and higher conversion (entries 6 and 14) when using *p*-chlorostyrene as substrate. In contrast, electron-withdrawing substituents (Cl, F) did not affect the reaction rate by using the established system [*t*BuC(NC₆H₃-*i*Pr₂-2,6)₂YbN(SiMe₃)₂(THF)] as catalyst.⁷² The hydrophosphination reaction of *p*-methylstyrene with 4 and 5 as catalysts does not show a clear tendency. The reaction of *p*-chlorostyrene with the divalent Yb compound 5 resulted in an immediate decomposition of the catalyst. We anticipate that the chlorine function of the substrate reacts with the Yb²⁺ atom.

In order to evaluate the enantioselectivity of the chiral amidinate catalysts, the hydrophosphination reaction of α -methylstyrene with Ph₂PH was investigated as a model reaction. The results are presented in Table S2. Because of the absence of a leaving group at the catalyst, the conversions were low to moderate. Only compound 3 showed a significantly higher conversion compared to the blank reaction. In the presence of 2.5 mol% of compound 3, the reaction reached a conversion of 60 % after 95 h at 100 °C (Table S2, entry 3). To determine the enantiomeric excess (ee) by ³¹P{¹H} NMR spectroscopy, the chiral derivatizing agent bis[{dimethyl(1-(2-naphthyl)ethyl)aminato-C²,N'}palladium(II)chloride], (*R*)-[Pd-{Me₂NCH(Me)C₁₀H₆}(μ-Cl)]₂,^{73,74} was added. Unfortunately, no clear results indicating an enantioselectivity were obtained.

CONCLUSION

Chiral homoleptic (S)-PEBA complexes of the heavier alkaline earth elements (M = Ca, Sr, Ba) and the divalent lanthanides (Ln = Eu²⁺, Yb²⁺) were synthesized. Three different structures are observed in the solid state. Compounds 1, 2, 4, and 5 form distorted coordination octahedra. For the alkaline earth element complexes, the two THF molecules are located in a *trans*-position, whereas, for the lanthanide compounds, they are arranged in a *cis*-position. In contrast, the barium complex 3 is dimeric with two amidinate ligands in an uncommon “side-on” bridging mode.

Although compounds 1–5 do not have a leaving group, they were used as catalysts in the hydrophosphination reaction of differently substituted styrenes and Ph₂PH. As a result of the low p*K*_a values of the phosphine, we do not anticipate a

substitution of one amidinate ligand by a phosphine during the catalytic transformation. Thus, a Lewis acid catalysis is suggested. Because of the absence of a leaving group, the catalytic activity of compounds 1–5 is lower compared to established systems. However, significant activity for some catalysts is observed. Within this series, the barium compound 3 showed the highest activity. This is in agreement with earlier observations, in which the activity increased with increasing ion radius of the center metal.^{46,63,66}

EXPERIMENTAL SECTION

General Methods. All air- and water-sensitive materials were prepared under a nitrogen atmosphere by using either a Schlenk line or a glovebox. THF was dried by distilling from potassium benzophenone ketyl under nitrogen before use. Toluene and *n*-pentane were obtained from a MBraun solvent purification system (SPS-800). Deuterated solvents were purchased from Carl Roth GmbH (99.5 atom % D) and were dried and stored in vacuum with Na/K alloy. NMR spectra were recorded on a Bruker Avance II 300 MHz spectrometer. Chemical shifts are referenced to internal solvent resonances and are reported relative to tetramethylsilane (¹H and ¹³C NMR), [Yb(C₅Me₅)₂(THF)₂] (¹⁷¹Yb NMR), respectively. Elemental analyses were carried out with an Elementar Vario Micro Cube. IR spectra were performed on a Bruker TENSOR 37 spectrometer via the attenuated total reflection method (ATR). [LnI₂(THF)₂]⁷⁵ and KCH(SiMe₃)₂⁷⁶ were prepared according to literature procedures.

[Ca(PEBA)₂(THF)₂] (1). (S)-HPEBA (0.40 g, 1.22 mmol) and KCH(SiMe₃)₂ (0.137 g, 1.22 mmol) were dissolved in toluene (10 mL) and then stirred at room temperature for 1 h. The solution was transferred to a suspension of CaI₂ (0.179 g, 0.61 mmol) in 10 mL of toluene. The resulting mixture was vigorously stirred overnight. Then, the solvent was removed under reduced pressure. The residue was dissolved in 20 mL of THF and stirred at room temperature for another 24 h. The solvent was directly removed *in vacuo*, and the residue was extracted with *n*-pentane (15 mL). The solution was concentrated to dryness. Finally, the remaining powder was dried under reduced pressure. The product was purified by recrystallization from a concentrated *n*-pentane solution. Yield: 204 mg (based on single crystals), 0.23 mmol, 38%. Anal. Calcd for C₅₉H₆₇N₄O₂Ca (904.28): C, 78.37, H, 7.47, N, 6.2. Found: C, 79.00, H, 6.63, N, 6.00. ¹H NMR (300.13 MHz, C₆D₆, 298 K): δ (ppm) = 7.52 (d, *J* = 7.0 Hz, 1H, Ph), 7.34 (d, *J* = 7.0 Hz, 8H, Ph), 7.23 (t, *J* = 7.4 Hz, 6H, Ph), 7.18–7.02 (m, 15H, Ph), 4.29 (q, *J* = 6.6 Hz, 4H, CH), 3.84–3.77 (m, 4H, CH₂(THF)), 3.73–3.57 (m, 4H, CH₂(THF)), 1.47 (d, *J* = 6.6 Hz, 12H, CH₃), 1.43–1.35 (m, 8H, CH₂(THF)). ¹³C{¹H} NMR (75.48 MHz, C₆D₆, 298 K): δ (ppm) = 174.5 (NCN), 150.7 (*i*-Ph), 139.2 (*i*-Ph), 127.8 (Ph), 127.0 (Ph), 126.8 (Ph), 126.7 (Ph), 125.3 (Ph), 68.4 (CH₂(THF)), 57.3 (CH), 27.2 (CH₃), 25.1 (CH₂(THF)); the signals for the quaternary carbon atoms were not observed. IR (ATR) ν (cm⁻¹): 3406 (s), 3317 (w), 2978 (w), 2953 (w), 2919 (w), 2875 (w), 1636 (vs), 1485 (s), 1447 (m), 1304 (m), 1266 (m), 1214 (w), 1141 (w), 1071 (w), 1028 (m), 763 (s), 700 (s), 544 (m).

[Sr(PEBA)₂(THF)₂] (2). Following the procedure described above for 1, the reaction of (S)-HPEBA (0.40 g, 1.22 mmol) and KCH(SiMe₃)₂ (0.137 g, 1.22 mmol) and SrI₂ (0.208 g, 0.61 mmol) afforded colorless crystals of 2. Yield: 150 mg (based on single crystals), 0.173 mmol, 28%. Anal. Calcd for C₅₃H₅₃N₄O₂Sr (865.64): C, 73.54, H, 6.17, N, 6.47. Found: 73.50, H, 6.62, N, 5.49. ¹H NMR (300.13 MHz, C₆D₆, 298 K): δ (ppm) = 7.40–7.28 (m, 8H, Ph), 7.25–6.70 (m, 22H, Ph), 4.29 (q, *J* = 6.2 Hz, 4H, CH), 3.74–3.63 (m, 4H, CH₂(THF)), 3.61–3.47 (m, 4H, CH₂(THF)), 1.48 (d, *J* = 6.7 Hz, 12H, CH₃), 1.41–1.36 (m, 8H, CH₂(THF)). ¹³C{¹H} NMR (75.48 MHz, C₆D₆, 298 K): δ (ppm) = 174.2 (NCN), 151.3 (*i*-Ph), 139.5 (*i*-Ph), 127.9 (Ph), 127.8 (Ph), 127.1 (Ph), 126.6 (Ph), 126.4 (Ph), 125.2 (Ph), 68.3 (CH₂(THF)), 57.6 (CH), 27.6 (CH₃), 25.6 (CH₂(THF)). IR (ATR) ν (cm⁻¹): 3406 (s), 3061 (w), 2977 (m), 2954 (m), 2921 (w), 2877 (w), 1636 (vs), 1599 (w), 1486 (s), 1448

(s), 1355 (w), 1303 (m), 1267 (m), 1211 (w), 1141 (w), 1071 (w), 1027 (m), 763 (s), 700 (s), 544 cm^{-1} (s).

[Ba(PEBA)₂]₂ (3). Following the procedure described above for 1. The reaction of (S)-HPEBA (0.40 g, 1.22 mmol), KCH(SiMe₃)₂ (0.137 g, 1.22 mmol), and BaI₂ (0.238 g, 0.61 mmol) afforded colorless crystals of 3.

Yield: 137 mg (based on single crystals), 0.083 mmol, 27%. Anal. Calcd for (1650.57): C₉₇H₉₈Ba₂N₈: C, 70.59, H, 6.79, N, 5.98. Found: C, 69.91, H, 5.74, N, 5.77. ¹H NMR (300.13 MHz, C₆D₆, 298 K): δ (ppm) = 7.21 (t, *J* = 7.7 Hz, 8H, Ph), 7.07–6.80 (m, 48H, Ph), 6.48–6.45 (m, 4H, Ph), 4.15 (q, *J* = 6.5 Hz, 4H, CH), 4.05 (q, *J* = 6.6 Hz, 4H, CH), 1.25 (d, *J* = 6.7 Hz, 12H, CH₃), 1.14 (d, *J* = 6.7 Hz, 12H, CH₃). ¹³C{¹H} NMR (75.48 MHz, C₆D₆, 298 K): δ (ppm) = 177.0 (NCN), 174.8 (NCN), 151.5 (*i*-Ph), 148.1 (*i*-Ph), 139.0 (*i*-Ph), 136.5 (*i*-Ph), 129.4 (Ph), 128.2 (Ph), 127.9 (Ph), 127.6 (Ph), 126.7 (Ph), 126.6 (Ph), 126.5 (Ph), 126.3 (Ph), 126.2 (Ph), 125.1 (Ph), 57.2 (CH), 56.9 (CH), 26.5 (CH₃), 25.9 (CH₃); the signals for the quaternary carbon atoms were not observed. IR (ATR) ν (cm^{-1}): 3406 (s), 3058 (w), 2954 (m), 2921 (s), 2876 (m), 1636 (vs), 1598 (w), 1485 (s), 1447 (s), 1303 (m), 1267 (m), 1211 (w), 1141 (w), 1071 (w), 1027 (m), 762 (s), 699 (s), 543 (s).

[Eu(PEBA)₂(THF)₂] (4). Following the similar procedure described above for 1. The reaction of (S)-HPEBA (0.40 g, 1.22 mmol), KCH(SiMe₃)₂ (0.137 g, 1.22 mmol), and EuI₂(THF)₂ (0.335 g, 0.61 mmol) afforded 4 as orange single crystals. Yield: 156 mg (based on single crystals), 0.164 mmol, 27%. Anal. Calcd for C₅₄H₆₂N₄O₂Eu (951.07): C, 68.2, H, 6.57, N, 5.89. Found: C, 67.94, H, 6.05, N, 6.21. IR (ATR) ν (cm^{-1}): 3405 (s), 3058 (w), 2976 (m), 2956 (m), 2920 (w), 2874 (w), 1635 (vs), 1598 (w), 1485 (s), 1447 (s), 1355 (w), 1303 (m), 1266 (m), 1210 (w), 1141 (w), 1071 (w), 1026 (m), 763 (s), 699 (s), 543 (s).

[Yb(PEBA)₂(THF)₂] (5). Following the similar procedure described above for 1. The reaction of (S)-HPEBA (0.40 g, 1.22 mmol), KCH(SiMe₃)₂ (0.137 g, 1.22 mmol), and YbI₂(THF)₂ (0.348, 0.61 mmol) afforded dark red crystals of 5. Yield: 121 mg (based on single crystals), 0.125 mmol, 20%. Anal. Calcd for C₅₄H₆₂N₄O₂Yb (972.15): C, 66.72, H, 6.43, N, 5.76. Found: C, 66.72, H, 6.09, N, 6.17. ¹H NMR (300.13 MHz, C₆D₆, 298 K): δ (ppm) = 7.37 (d, *J* = 7.5 Hz, 8H, Ph), 7.24–7.00 (m, 22H, Ph), 4.40 (q, *J* = 6.7 Hz, 4H, CH), 3.69 (br s, 4H, CH₂(THF)), 3.60 (br s, 4H, CH₂(THF)), 1.48 (d, *J* = 6.6 Hz, 12H, CH₃), 1.39 (br s, 8H, CH₂(THF)). ¹³C{¹H} NMR (75.48 MHz, C₆D₆, 298 K): δ (ppm) = 174.4 (NCN), 150.9 (*i*-Ph), 139.4 (*i*-Ph), 127.8 (Ph), 127.0 (Ph), 126.8 (Ph), 126.7 (Ph), 125.2 (Ph), 68.2 (CH₂(THF)), 57.2 (CH), 27.0 (CH₃), 25.2 (CH₂(THF)). ¹⁷¹Yb{¹H} NMR (52.5 MHz, C₆D₆, 298 K): 792 ppm. IR (ATR) ν (cm^{-1}): 3406 (s), 3058 (w), 3024 (w), 2955 (s), 2921 (vs), 2855 (s), 1635 (vs), 1598 (m), 1485 (s), 1448 (s), 1355 (w), 1303 (m), 1265 (m), 1211 (w), 1140 (w), 1070 (w), 1026 (m), 762 (s), 699 (s), 542 (s).

X-ray Crystallographic Studies of 1–5. A suitable crystal was covered in mineral oil (Aldrich) and mounted on a glass fiber. The crystal was transferred directly to a cold stream of a STOE IPDS 2 or STOE StadiVari diffractometer.

All structures were solved using SHELXS/T-2014.^{77–79} The remaining non-hydrogen atoms were located from successive difference Fourier map calculations. The refinements were carried out by using full-matrix least-squares techniques on *F*, minimizing the function ($F_o - F_c$)², where the weight is defined as $4F_o^2/2(F_o^2)$ and F_o and F_c are the observed and calculated structure factor amplitudes using the program SHELXL-2014.⁷⁷ Hydrogen atom positions were calculated. The locations of the largest peaks in the final difference Fourier map calculation as well as the magnitude of the residual electron densities in each case were of no chemical significance. Positional parameters, hydrogen atom parameters, thermal parameters, and bond distances and angles have been deposited as Supporting Information. Data collection parameters and selected bond lengths and angles are given in Table S1 and the corresponding figure captions.

■ ASSOCIATED CONTENT

Supporting Information

The Supporting Information is available free of charge on the ACS Publications website at DOI: 10.1021/acs.organomet.6b00373.

Experimental procedures and NMR spectra (PDF)

Crystallographic data of compounds 1–5 (CIF)

■ AUTHOR INFORMATION

Corresponding Author

*E-mail: roesky@kit.edu.

Notes

The authors declare no competing financial interest.

■ ACKNOWLEDGMENTS

This work was supported by the DFG-funded transregional collaborative research center SFB/TRR 88 “3MET”. This work was also supported by the Landesstiftung Baden-Württemberg gGmbH and the KIT. M.H. gratefully acknowledges a grant from the China Scholarship Council (No. 201206250015).

■ REFERENCES

- Trifonov, A. A. *Coord. Chem. Rev.* **2010**, 254, 1327–1347.
- Chlupaty, T.; Ruzicka, A. *Coord. Chem. Rev.* **2016**, 314, 103–113.
- Junk, P. C.; Cole, M. L. *Chem. Commun.* **2007**, 1579–1590.
- Edelmann, F. T. *Coord. Chem. Rev.* **1994**, 137, 403–481.
- Edelmann, F. T. *Angew. Chem., Int. Ed. Engl.* **1995**, 34, 2466–88.
- Edelmann, F. T. *Top. Curr. Chem.* **1996**, 179, 113–148.
- Edelmann, F. T. *Advances in the Coordination Chemistry of Amidinate and Guanidinate Ligands*. In *Advanced Organometallic Chemistry*; Anthony, F. H., Mark, J. F., Eds.; Academic Press: San Diego, CA, 2008; Chapter 3, Vol. 57, pp 183–352.
- Milanov, A. P.; Fischer, R. A.; Devi, A. *Inorg. Chem.* **2008**, 47, 11405–11416.
- Edelmann, F. T. *Chem. Soc. Rev.* **2009**, 38, 2253–2268.
- Edelmann, F. T. *Struct. Bonding (Berlin, Ger.)* **2010**, 137, 109–163.
- Edelmann, F. T. *Chem. Soc. Rev.* **2012**, 41, 7657–7672.
- Wedler, M.; Knösel, F.; Pieper, U.; Stalke, D.; Edelmann, F. T.; Amberger, H.-D. *Chem. Ber.* **1992**, 125, 2171–2181.
- Cole, M. L.; Deacon, G. B.; Forsyth, C. M.; Junk, P. C.; Konstas, K.; Wang, J.; Bittig, H.; Werner, D. *Chem.—Eur. J.* **2013**, 19, 1410–1420.
- Cole, M. L.; Junk, P. C. *Chem. Commun.* **2005**, 2695–2697.
- Cole, M. L.; Deacon, G. B.; Junk, P. C.; Konstas, K. *Chem. Commun.* **2005**, 1581–1583.
- Cole, M. L.; Deacon, G. B.; Forsyth, C. M.; Junk, P. C.; Konstas, K.; Wang, J. *Chem.—Eur. J.* **2007**, 13, 8092–8110.
- Westerhausen, M.; Hausen, H. D.; Schwarz, W. Z. *Anorg. Allg. Chem.* **1992**, 618, 121–130.
- Westerhausen, M.; Schwarz, W. Z. *Anorg. Allg. Chem.* **1993**, 619, 1455–1461.
- Westerhausen, M.; Schwarz, W. Z. *Naturforsch., B: J. Chem. Sci.* **1992**, 47, 453–459.
- Hu, H.; Cui, C. *Organometallics* **2012**, 31, 1208–1211.
- Glock, C.; Loh, C.; Görls, H.; Kriek, S.; Westerhausen, M. *Eur. J. Inorg. Chem.* **2013**, 2013, 3261–3269.
- Loh, C.; Seupel, S.; Görls, H.; Kriek, S.; Westerhausen, M. *Eur. J. Inorg. Chem.* **2014**, 2014, 1312–1321.
- Cole, M. L.; Junk, P. C. *New J. Chem.* **2005**, 29, 135–140.
- Cole, M. L.; Deacon, G. B.; Forsyth, C. M.; Konstas, K.; Junk, P. C. *Dalton Trans.* **2006**, 3360–3367.
- Averbuj, C.; Tish, E.; Eisen, M. S. *J. Am. Chem. Soc.* **1998**, 120, 8640–8646.

- (26) Koterwas, L. A.; Fetting, J. C.; Sita, L. R. *Organometallics* **1999**, *18*, 4183–4190.
- (27) Li, J.; Huang, S.; Weng, L.; Liu, D. *J. Organomet. Chem.* **2006**, *691*, 3003–3010.
- (28) Ward, B. D.; Risler, H.; Weitershaus, K.; Bellemin-Laponnaz, S.; Wade, P. H.; Gade, L. H. *Inorg. Chem.* **2006**, *45*, 7777–7787.
- (29) Brunner, H.; Lukasek, J.; Agrifoglio, G. *J. Organomet. Chem.* **1980**, *195*, 63–76.
- (30) Nelkenbaum, E.; Kapon, M.; Eisen, M. S. *J. Organomet. Chem.* **2005**, *690*, 3154–3164.
- (31) Bertogg, A.; Togni, A. *Organometallics* **2006**, *25*, 622–630.
- (32) Brunner, H.; Agrifoglio, G. *Monatsh. Chem.* **1980**, *111*, 275–287.
- (33) Benndorf, P.; Preuß, C.; Roesky, P. W. *J. Organomet. Chem.* **2011**, *696*, 1150–1155.
- (34) Benndorf, P.; Jenter, J.; Zielke, L.; Roesky, P. W. *Chem. Commun.* **2011**, *47*, 2574–2576.
- (35) Benndorf, P.; Kratsch, J.; Hartenstein, L.; Preuss, C. M.; Roesky, P. W. *Chem.—Eur. J.* **2012**, *18*, 14454–14463.
- (36) Kratsch, J.; Kuzdrowska, M.; Schmid, M.; Kazeminejad, N.; Kaub, C.; Oña-Burgos, P.; Guillaume, S. M.; Roesky, P. W. *Organometallics* **2013**, *32*, 1230–1238.
- (37) Delacroix, O.; Gaumont, A. C. *Curr. Org. Chem.* **2005**, *9*, 1851–1882.
- (38) Beletskaya, I. P.; Ananikov, V. P.; Khemchyan, L. L. Synthesis of Phosphorus Compounds via Metal-Catalyzed Addition of P–H Bond to Unsaturated Organic Molecules. In *Phosphorus Compounds: Advanced Tools in Catalysis and Material Sciences*; Peruzzini, M., Gonsalvi, L., Eds.; Springer: Dordrecht, Netherlands, 2011; pp 213–264.
- (39) Rosenberg, L. *ACS Catal.* **2013**, *3*, 2845–2855.
- (40) Waterman, R. *Dalton Trans.* **2009**, 18–26.
- (41) Douglass, M. R.; Marks, T. J. *J. Am. Chem. Soc.* **2000**, *122*, 1824–1825.
- (42) Douglass, M. R.; Stern, C. L.; Marks, T. J. *J. Am. Chem. Soc.* **2001**, *123*, 10221–10238.
- (43) Kawaoka, A. M.; Douglass, M. R.; Marks, T. J. *Organometallics* **2003**, *22*, 4630–4632.
- (44) Motta, A.; Fragalà, I. L.; Marks, T. J. *Organometallics* **2005**, *24*, 4995–5003.
- (45) Takaki, K.; Komeyama, K.; Takehira, K. *Tetrahedron* **2003**, *59*, 10381–10395.
- (46) Liu, B.; Roisnel, T.; Carpentier, J.-F.; Sarazin, Y. *Chem.—Eur. J.* **2013**, *19*, 13445–13462.
- (47) Wang, F.; Wang, S.; Zhu, X.; Zhou, S.; Miao, H.; Gu, X.; Wei, Y.; Yuan, Q. *Organometallics* **2013**, *32*, 3920–3931.
- (48) Behrle, A. C.; Schmidt, J. A. R. *Organometallics* **2013**, *32*, 1141–1149.
- (49) Kissel, A. A.; Mahrova, T. V.; Lyubov, D. M.; Cherkasov, A. V.; Fukin, G. K.; Trifonov, A. A.; Del Rosal, I.; Maron, L. *Dalton Trans.* **2015**, *44*, 12137–12148.
- (50) Basalov, I. V.; Dorcet, V.; Fukin, G. K.; Carpentier, J.-F.; Sarazin, Y.; Trifonov, A. A. *Chem.—Eur. J.* **2015**, *21*, 6033–6036.
- (51) Gu, X.; Zhang, L.; Zhu, X.; Wang, S.; Zhou, S.; Wei, Y.; Zhang, G.; Mu, X.; Huang, Z.; Hong, D.; Zhang, F. *Organometallics* **2015**, *34*, 4553–4559.
- (52) Basalov, I. V.; Yurova, O. S.; Cherkasov, A. V.; Fukin, G. K.; Trifonov, A. A. *Inorg. Chem.* **2016**, *55*, 1236–1244.
- (53) Molander, G. A.; Romero, J. A. C. *Chem. Rev.* **2002**, *102*, 2161–2186.
- (54) Mei, L. *Lett. Org. Chem.* **2008**, *5*, 174–190.
- (55) Reznichenko, A. L.; Hultsch, K. C. *Struct. Bonding (Berlin, Ger.)* **2010**, *137*, 1–48.
- (56) Rodriguez-Ruiz, V.; Carlino, R.; Bezenine-Lafollee, S.; Gil, R.; Prim, D.; Schulz, E.; Hannedouche, J. *Dalton Trans.* **2015**, *44*, 12029–12059.
- (57) Wathier, M.; Love, J. A. *Eur. J. Inorg. Chem.* **2016**, *2016*, 2391.
- (58) Eaborn, C.; Hitchcock, P. B.; Izod, K.; Lu, Z.-R.; Smith, J. D. *Organometallics* **1996**, *15*, 4783–4790.
- (59) Harder, S. *Angew. Chem., Int. Ed.* **2004**, *43*, 2714–2718.
- (60) Schumann, H.; Schutte, S.; Kroth, H.-J.; Lentz, D. *Angew. Chem., Int. Ed.* **2004**, *43*, 6208–6211.
- (61) Weber, F.; Sitzmann, H.; Schultz, M.; Sofield, C. D.; Andersen, R. A. *Organometallics* **2002**, *21*, 3139–3146.
- (62) Greenwood, N. N.; Earnshaw, A. *Chemistry of the Elements*; Pergamon Press: Oxford, U.K., 1984; pp 122 and 1430.
- (63) Hill, M. S.; Liptrot, D. J.; Weetman, C. *Chem. Soc. Rev.* **2016**, *45*, 972–988.
- (64) Crimmin, M. R.; Barrett, A. G. M.; Hill, M. S.; Hitchcock, P. B.; Procopiou, P. A. *Organometallics* **2007**, *26*, 2953–2956.
- (65) Crimmin, M. R.; Hill, M. S. Homogeneous Catalysis with Organometallic Complexes of Group 2. In *Alkaline-Earth Metal Compounds: Oddities and Applications*; Harder, S., Ed.; Springer: Berlin, 2013; pp 191–241.
- (66) Liu, B.; Roisnel, T.; Carpentier, J.-F.; Sarazin, Y. *Angew. Chem., Int. Ed.* **2012**, *51*, 4943–4946.
- (67) Arrowsmith, M.; Crimmin, M. R.; Hill, M. S.; Lomas, S. L.; Heng, M. S.; Hitchcock, P. B.; Kociok-Kohn, G. *Dalton Trans.* **2014**, *43*, 14249–14256.
- (68) Cameron, T. M.; Xu, C.; Dipasquale, A. G.; Rheingold, A. L. *Organometallics* **2008**, *27*, 1596–1604.
- (69) Yao, S.; Chan, H.-S.; Lam, C.-K.; Lee, H. K. *Inorg. Chem.* **2009**, *48*, 9936–9946.
- (70) Heitmann, D.; Jones, C.; Junk, P. C.; Lippert, K.-A.; Stasch, A. *Dalton Trans.* **2007**, 187–189.
- (71) Heitmann, D.; Jones, C.; Mills, D. P.; Stasch, A. *Dalton Trans.* **2010**, *39*, 1877–1882.
- (72) Basalov, I. V.; Roşca, S. C.; Lyubov, D. M.; Selikhov, A. N.; Fukin, G. K.; Sarazin, Y.; Carpentier, J.-F.; Trifonov, A. A. *Inorg. Chem.* **2014**, *53*, 1654–1661.
- (73) Chooi, S. Y. M.; Leung, P.-h.; Chin Lim, C.; Mok, K. F.; Quek, G. H.; Sim, K. Y.; Tan, M. K. *Tetrahedron: Asymmetry* **1992**, *3*, 529–532.
- (74) Xu, C.; Jun Hao Kennard, G.; Hennersdorf, F.; Li, Y.; Pullarkat, S. A.; Leung, P.-H. *Organometallics* **2012**, *31*, 3022–3026.
- (75) Dahlén, A.; Hilmersson, G. *Eur. J. Inorg. Chem.* **2004**, *2004*, 3020–3024.
- (76) Hitchcock, P. B.; Khvostov, A. V.; Lippert, M. F. *J. Organomet. Chem.* **2002**, *663*, 263–268.
- (77) Sheldrick, G. M. *Acta Crystallogr., Sect. A: Found. Crystallogr.* **2008**, *64*, 112–122.
- (78) Sheldrick, G. M. *Acta Crystallogr., Sect. A: Found. Adv.* **2015**, *71*, 3–8.
- (79) Sheldrick, G. M. *Acta Crystallogr., Sect. C: Struct. Chem.* **2015**, *71*, 3–8.